JOURNAL OF THE TENNESSEE ACADEMY OF SCIENCE 86(2):56–62 JUNE 2011

UNCONFINED COMPRESSIVE STRENGTH OF SHALE AS A FUNCTION OF PETROPHYSICAL PROPERTIES: A CASE STUDY FROM EASTERN TENNESSEE

ARPITA NANDI AND RACHEL CONDE

Department of Geosciences, East Tennessee State University, Johnson City, TN 37614 (Email: nandi@etsu.edu)

ABSTRACT—Unconfined compressive strength (UCS) is a fundamental property used for design purposes in civil, mining, and petroleum engineering. Determination of UCS of shale is difficult because of the problem of proper sample preparation and expensive test procedures. This paper presents the mineralogical and physical properties, investigates the relationships among them, and attempts to derive a reliable empirical model for estimating UCS. The study was performed using samples from Sevier Shale of eastern Tennessee, a part of the Valley and Ridge Province. The samples were tested for bulk rock mineralogy using the X-ray diffraction method. Microfracture density analysis was performed from thin sections using image analysis software. Physical properties (specific gravity, moisture content, porosity, and microfracture density) were determined, and strength was measured in terms of UCS using a point load test. UCS of Sevier Shale ranged from 0.53 MPa (1410.13 psi) for weathered, more fissile shales to 73.30 MPa (9064.38 psi) for more coherent rocks. The results were statistically described and analyzed using backward multiple regression technique. Strong statistical correlation was found between UCS, clay content, porosity, microfracture density, and specific gravity of the shale samples. The presence of microfractures filled with clay and calcite significantly affected the strength of the rock mass. Overall porosity was low and related to the microfracture density.

Estimation of the strength of shale is of great interest to geologists, as well as civil, mining, and petroleum engineers, involved in various design projects. Among the different strength parameters, Unconfined Compressive Strength (UCS) is most frequently used in rock mechanics and is usually determined through a laboratory test. Although the UCS test is relatively simple, it is expensive, time-consuming, and requires meticulous sample preparation. For weak rocks like shale, further difficulties arise concerning good quality sample collection, either from a field outcrop or a drill core. The general tendency among practitioners is to estimate UCS of shale using simpler, quicker, and less expensive procedures, such as Point Load, Schmidt Hammer Rebound, and Sonic Velocity tests (Kahraman, 2001)

Petrographic and physical features including structure, texture, and mineral composition of shale are intrinsic properties that control the UCS of the rock (Hoek and Brown, 1997; Singh, 2001). Several investigations on various rock types have been executed which include predicting UCS using durability, hardness, structural properties, friction angle (Yasar and Erdogan, 2004; Shalabi et al., 2007); and using rock type, velocity, Young's modulus, porosity, and grain density (Gokceoglu and Aksoy, 2000; Kahraman, 2001; Chang et al., 2006; Santi, 2006). Few studies have emphasized lithological characters, like degree of induration, grain size distribution, mineralogical composition, and degree of micro-fracturing (Dick and Shakoor, 1992; Horsrud, 2001; Gemici, 2001). However, research on shale rock mechanics based on mineralogy, structure, and physical behavior is meager. This paper deals with the application of multivariate statistical analysis for the prediction of UCS from mineral composition, microfractures, porosity, specific gravity, and moisture content of shale.

BACKGROUND GEOLOGY

A complex mosaic of weathered Ordovician aged Sevier Shale is widely distributed throughout the sedimentary sequences in the southern Appalachians. Sevier Shale is a blue-gray silty to sandy, calcareous shale. In many sections it is also strongly carbonaceous. It was named by Hayes (1891) for a wide belt of exposed shale in Sevier County, Tennessee. Sevier Shale overlays the Knox Group carbonates and underlies the Bays Formation. The minimum stratigraphic thickness is reported as 800 m (2,500 ft) in the Bays Mountain synclinorium and the maximum is 2,300 m (7,000 ft) in Blount and Monroe counties (Rodgers, 1953; Shanmugam and Walker, 1983).

Sevier Shale occurs as folded and faulted sequences within the fold and thrust belt. Structurally, this shale acts as decollement surfaces and serves as the dominant glide plane surface for thrust faults in the region. Road-cut exposures commonly exhibit multiple cleavage directions and calcite veining. Sevier Shale include relatively large amounts of organic material, thus acting as a potential hydrocarbon source rock in some parts of the region. Its fine-grained texture and low permeability allow this rock to form a good reservoir cap rock. Surface exposures weather to a yellow friable unit or yellow clays (Rodgers, 1953). Sevier Shale produces graptolites, sometimes pyritized, trilobites, and brachiopods. Secondary pyrite growth, gypsum growth, and calcite veining are ubiquitous, and exposed sequences weather to friable and unstable slopes, and, ultimately, to soil. It is interpreted as a sequence dominated by deep water marine sediments deposited in a forearc basin environment (Rodgers, 1953). The presence of carbonates, minor sands, and conglomerates clearly

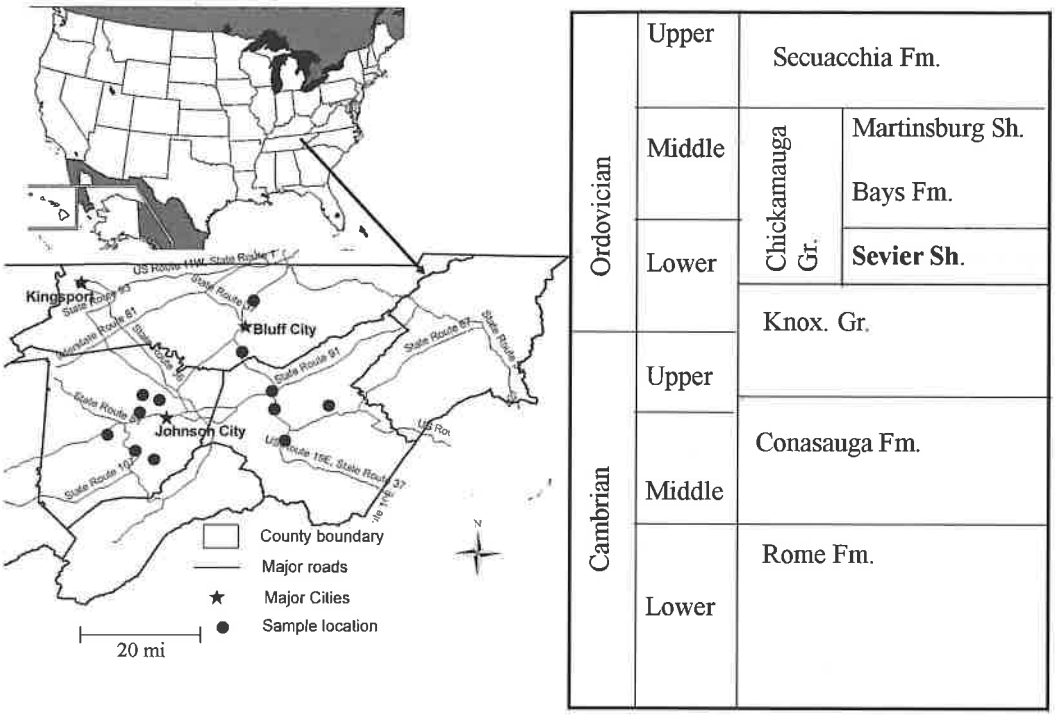

FIG. 1. Sampling location map and a simplified stratiraphic column of eastern Tennessee.

indicates a more complex depositional history which suggests a shallow water influence. These sequences are exposed over a large area of east Tennessee; therefore, understanding the shale engineering characteristics as building material is important.

RESEARCH METHODS AND RESULTS

A total of thirty-five shale samples (from twelve locations of Sevier Shale) were collected from various rock exposures and road cuts (Fig. 1). Relatively fresh block samples were collected in the field by first removing the weathered soil. Block samples were then extracted from the outcrop using a hammer and chisel, and care was taken to avoid creating additional fractures in the shale during collection and transportation to the laboratory. The laboratory procedures included X-ray diffraction, photomicrograph image analysis, specific gravity, moisture content, porosity and unconfined compressive strength determination. For quality control assessment of the laboratory tests, selected shale samples were sent to a commercial external laboratory for comparison of the results (Table 1).

X-ray diffraction (XRD) analysis was performed on powdered shale samples in order to assess the whole rock mineralogy. Samples were analyzed on a Shimadzu XRD 6000 diffractometer run at 40.0 kV and 30.0 mA. The data were collected from 05° to 45° 2-theta with a continuous scan of 2.0°/min and 0.02° sampling pitch. XRD analysis revealed that Sevier Shale is composed of quartz, orthoclase, microcline, calcite, gypsum, chlorite, illite, and mixed layers of kaolinite–montmorillonite (Fig. 2). Of the four types of clay minerals, montmorillonite is a smectitic (expanding) clay. The whole-rock quantitative analysis including silicates, carbonates, sulfates, and total clay minerals is shown (Table 1). Using internal standard (quartz) of known quantity, the abundance of the major minerals was estimated quantitatively. The amount of total clay minerals ranged from 25% to 66%, averaging 47.9%. Due to sporadic appearance of quartz and feldspars (orthoclase and microcline), their abundance was calculated collectively, with an average of 43.83%. Calcite was the next dominant mineral phase and was present in 19 shale samples with an average of 7.22% (range = 0%–23%). Samples 2, 21, and 23 were sent to an external laboratory for XRD analysis, and the results were comparable (Table 1).

The microfracture density of the shale samples was observed in thin sections in crossed polarized light under a petrographic microscope (Figs. 3a–b). The traces of microfractures were prominent under a microscope view, which was often filled with secondary minerals like clay and calcite. The microfractures commonly followed the shale laminations; however, several of them were oriented randomly. To estimate the microfracture density, the photomicrographs of the thin sections were analyzed using image analysis software (ImageJ, developed by NIH). A representative rectangular quadrant was chosen from each thin section, and the area of interest was measured (in pixels) by the software measuring utility (Figs. 3c–d). The area was enhanced by using filters to emphasize the contrast between the microfractures and the surrounding matrix, and then the microfracture area was measured in pixels. The microfracture area was divided by the total area of the quadrant to give percent microfracture density, which averaged 18% (range = 8%–28%).

Specific gravity, moisture content, and porosity, critical characteristics of shale, were measured. Specific gravity was estimated using American Society for Testing and Materials standard method C 642 (ASTM, 1996). Using ASTM D2216, the moisture content of shale was determined and expressed as a percentage of the ratio of the weight of water to the weight of solids in a given rock sample. Conventional water saturation

TABLE 1. Results of X-ray diffraction, microfracture density, porosity, specific gravity, moisture content, and unconfined compressive strength tests for thirty-five Sevier Shale samples.

	Independent variables								Dependent variable	
	Chemical characters				Physical characters					
	% clay	% calcite	% gypsum	% quartz +feldspar	% Porosity	Specific Gravity	% moisture content	% microfrac. density	UCS in psi	UCS in MPa
Sample 1	66	6	3	25	18	2.60	5.89	28	3570 (3124)	25 (22)
Sample 2	65 (58)	18 (16)	2 (2)	15 (24)	15 (11)	2.47 (2.58)	8 (7.89)	25	2632	18
Sample 3	64	0	0	36	16	2.22	8.17	24	1410	10
Sample 4	60	0	0	40	15	2.65	6.33	23	6659 (6254)	46 (43)
Sample 5	58	13	0	29	16	2.70	4.17	25	6349	44
Sample 6	56	13	0	31	15	2.66	7.80	21	2330 (2448)	16 (17)
Sample 7	59	12	4	25	11	2.63	6.50	18	4395	30
Sample 8	60	13	0	27	12	2.64	6.50	18	3658	25
Sample 9	51	16	0	34	11	2.66	8.83	15	3284	23
Sample 10	52	0	0	48	15	2.69	8.10	19	4677	32
Sample 11	47	0	0	53	12	2.66	6.03	18	8102 (10584)	55 (73)
Sample 12	48	0	0	52	12	2.63	5.57	16	9819 (10176)	67 (70)
Sample 13	46	0	0	54	10	2.68	8.17	19	7596	52
Sample 14	45	0	0	55	12	2.54	7.83	19	7287	50
Sample 15	47	0	0	54	9	2.55	8.27	18	4018 (3230)	29 (22)
Sample 16	49	0	0	51	11	2.71	8.67	20	3915 (4614)	26 (32)
Sample 17	49	6	0	45	10	2.73	8.23	19	3719	26
Sample 18	52	6	0	42	15	2.57	5.20	25	3257 (3098)	22 (21)
Sample 19	48	9	0	43	13	2.65	4.73	15	5130 (5411)	34 (37)
Sample 20	49	11	1	39	14	2.61	5.13	21	3785	26
Sample 21	46 (52)	19 (15)	4 (6)	31 (27)	11 (9)	2.67 (2.71)	7.69 (7.56)	20	6166 (6096)	42 (42)
Sample 22	51	19	6	24	8	2.66	8.90	19	3263	22
Sample 23	37 (32)	23 (34)	5 (0)	35 (44)	9 (6)	2.72 (2.77)	8.35 (8.34)	16	6815	47
Sample 24	41	15	3	41	12	2.66	7.33	16	3706	26
Sample 25	51	6	0	43	11	2.57	5.20	15	3341 (2675)	23 (18)
Sample 26	25	0	0	75	7	2.66	6.03	18	7592	52
Sample 27	28	0	0	72	5	2.63	5.57	15	9064	62
Sample 28	46	20	2	32	11	2.47	8.00	11	2769	19
Sample 29	38	0	0	62	9	2.22	8.17	15	2362	16
Sample 30	38	0	0	62	10	2.54	7.83	13	7639	53
Sample 31	33	0	0	67	8	2.67	8.12	11	7674	53
Sample 32	35	0	0	65	5	2.55	7.42	19	7262	50
Sample 33	52	0	0	48	9	2.21	8.08	15	1456	10
Sample 34	36	9	0	55	5	2.71	4.17	9	6241	43
Sample 35	49	20	6	25	6	2.68	9.00	8	3352	23
Mean	47.77	6.03	0.80	45.41	11.05	2.59	7.00	18	4916	34
Max	66.00	20.00	6.20	75.00	18.00	2.73	9.00	28	9064	62
Min	25.00	0.00	0.00	23.60	5.00	2.21	4.17	8	1410	10
St. Dev.	9.78	7.02	1.74	14.46	3.42	0.14	1.47	5	2280	16

For independent variables, data in parentheses were taken from external laboratory results; for dependent variable, data in parentheses were taken from TDOT reports.

methods were used to determine the total porosity of shale samples (ISRM, 1985). The average moisture content of the shale samples was 7.09% (range = 4.17%–9.00%; Table 1). The average specific gravity was 2.60, a result that was largely consistent except for few samples with lower values. The total shale porosity values ranged from 5% to 18%, averaging 11.1%. Samples 2, 21, and 23 were sent in external laboratory for testing, and the results are given in parentheses (Table 1).

The UCS of Sevier Shale was evaluated using a Point Load test. The equipment is comprised of a loading frame that measures the force necessary to split the sample and a scale that measures the distance between the two contact loading

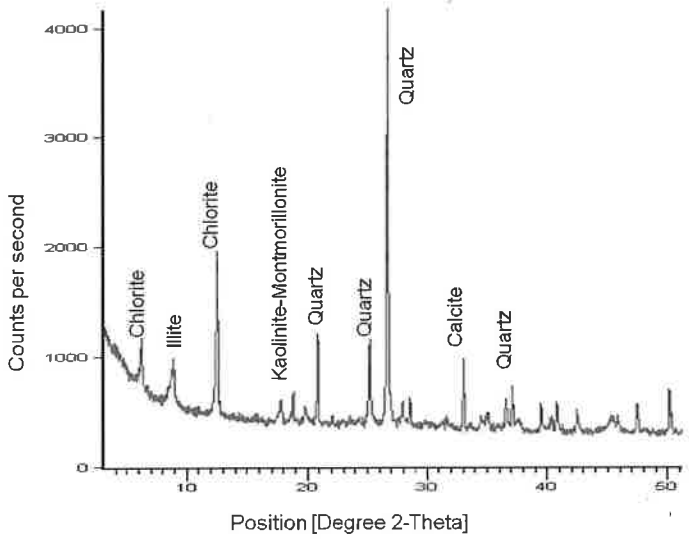

FIG. 2. X-ray Diffractogram of a representative shale sample.

points (Broch and Franklin, 1972). Irregular block samples were used to determine the Point Load Index (PLI), and then it was size-corrected to obtain the standard equivalent diameter (Sonmez and Osman, 2008). The UCS of the rock samples can be reasonably estimated by multiplying the PLI value by a conversion factor that can range from as low as 8 to as high as 35 (Brown, 1981). Research from Appalachian Shale (West Virginia) by Vallejo et al. (1993) has indicated a conversion factor of 12 to estimate UCS. UCS test data on Sevier Shale from several geotechnical projects by Tennessee Department of Transportation (TDOT) were used to select a suitable conversion factor for this study (Table 1). A sensitivity analysis was performed using a range of conversion factors (11 through 15), and 13 seemed to be the most suitable fit with TDOT UCS data. The UCS derived from PLI value for Sevier Shale ranged from 10.53 MPa (1410.13 psi) for weathered, more fissile shales to 73.30 MPa (9064.38 psi) for more coherent samples, with an overall average value of 37.17 MPa (4916.19 psi). According to the classification scheme of Marinos and Hoek (2006), UCS values of Sevier Shale are classified in the Weak, Medium Strong, and Strong categories.

Statistical Analysis

A multiple linear regression was performed on the dataset of 35 shale samples using general statistical program SPSS. Backward elimination process was used to develop a linear model to predict UCS from the independent variables (clay, calcite, gypsum, quartz, and feldspar content, porosity, specific gravity, moisture content, and microfracture density). In four consecutive steps the backward multiple regression predicted the most suitable model for the data. Accuracy of the four different models was calculated by multiple determination coefficient R, and square of multiple determination coefficient R^2. The closer R and R^2 to unity, the better the model fits the data. In the study, R and R^2 values gradually increased from step 1 to step 4 for the backward regression (Table 2). Standard estimate of error was calculated which diminished with elimination of insignificant variables.

The multiple regression models to predict UCS were started by including all of the dependent variables (Table 2). However, all the variables did not survive the backward elimination process under the given constraints of confidence interval (95%) and significance values and were excluded during elimination. The insignificant variables included calcite, gypsum, quartz and feldspar, and moisture content. The final model (in step 4) was composed of significant variables, such as clay content, porosity, specific gravity, and microfracture density (Table 2). The "variable" column in Table 2 showed all the independent variables and the constant term (Y intercept) of the regression equation. "B" included the values for the regression equation for predicting the dependent variable from the independent variables (coefficients). The *P*-

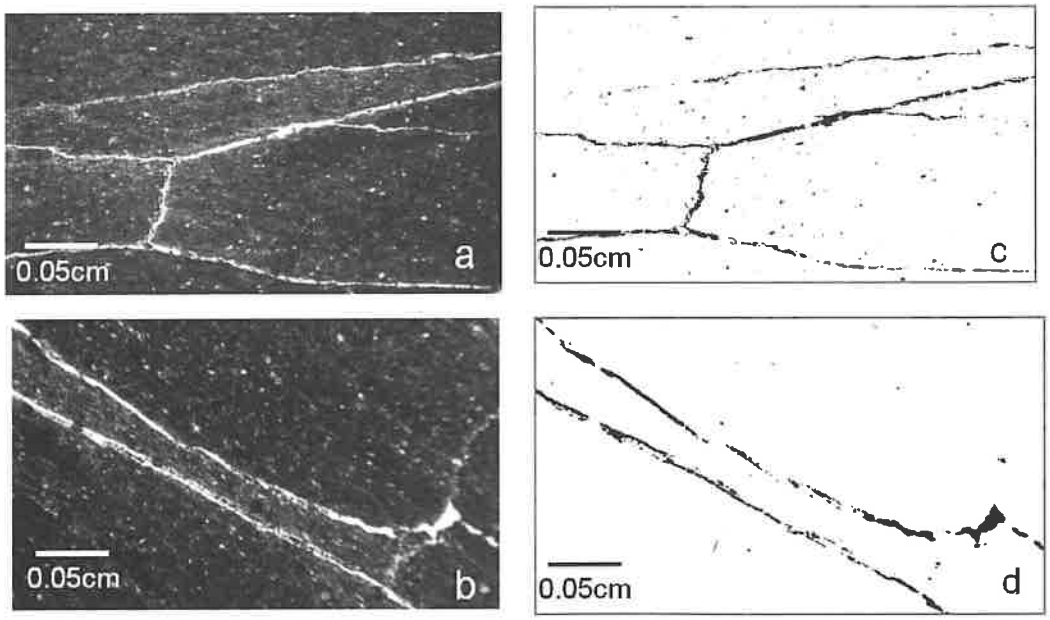

FIG. 3a–d. Petrographic thin section of shale sample 5 and 6 in crossed polarized light (a and b) and corresponding images of microfractures filtered by image processing software (c and d).

TABLE 2. Models derived from the backward multivariate regression result.

Model	Variables	B	Std. Error	Sig.	R	R^2	Std. estimate of error
1	(Constant)	213.427	29.730	.000	0.65	0.39	18.10
	clay	−.571	.211	.012			
	calcite	.057	.247	.820			
	gypsum	2.176	1.034	.045			
	quartz and feldspar	1.356	0.851	.623			
	porosity	−139.818	71.484	.061			
	specific gravity	36.746	9.938	.052			
	moisture content	−1.886	.941	.055			
	microfracture density	−152.637	40.623	.001			
2	(Constant)	212.343	28.853	.000	0.75	0.57	12.44
	clay	−.563	.205	.010			
	gypsum	2.343	.726	.003			
	porosity	−136.910	69.155	.058			
	specific gravity	36.250	9.536	.046			
	moisture content	−1.907	.920	.048			
	microfracture density	−155.531	37.963	.000			
3	(Constant)	180.346	31.182	.000	0.85	0.73	8.10
	clay	−.352	.224	.016			
	porosity	−188.632	77.419	.021			
	specific gravity	26.833	10.448	.031			
	moisture content	−1.054	1.015	.308			
	microfracture density	−158.016	43.681	.001			
4	(Constant)	167.247	28.556	.000	0.90	0.81	7.01
	clay	−.404	.218	.014			
	porosity	−168.863	75.142	.021			
	specific gravity	24.661	10.250	.032			
	microfracture density	−156.365	43.710	.001			

values (significance) were used in testing, and higher P-values were excluded from the iteration (Table 2). For the final model in step 4, the regression equation (Equation 1) is:

$$UCS_{MPa} = 167.247 - 0.404\ clay\ content - 168.863\ porosity + 24.661\ specific\ gravity - 156.365\ Microfracture\ density \quad (1)$$

The residuals from the regression model were examined using (1) Normal probability-probability (P-P) plot and (2) Scatterplot (Figs. 4a and 4b). P-P plot is a method of testing if the residuals from the regression are normally distributed. A close proximity of the dots to the 45° line in P-P plot (Fig. 4a) with the residuals balanced evenly around the zero line in the scatterplot (Fig. 4b) indicated an overall good fit of the data to the model.

Influence of Mineralogical and Physical Properties on UCS

In the study, XRD results indicate that Sevier Shale is composed of quartz, calcite, chlorite, gypsum, pyrite, illite, and mixed layer kaolinite–montmorillonite. The data analysis did not show any significant statistical correlation of quartz, feldspar, and calcite with the UCS of shale. However, the regression model indicates that a strong relationship exists between UCS and abundance of clay minerals. The clay minerals are concentrated in the rock matrix. The thin section and image analysis results show that additional clay minerals and microscopic calcite crystals are present in Sevier Shale microfractures and are likely to be deposited when groundwater flows through the fractured shale. Clay minerals are soft, hygroscopic, and prone to swelling, and calcite is relatively soft and soluble. Thus, presence of clay and calcite significantly affect the UCS of a rock.

In addition to overall mineralogy, it is also important to consider the rock microfabric and physical behavior when evaluating the shale for engineering design purposes. The total porosity of the shale samples in the research area is generally low. The UCS of the shale decreases with the increased porosity and hence shows a negative trend. The presence of microfractures can lead to variation in porosity, and as a result, rock mechanical properties changes. A direct relationship between porosity and microfracture density is common; however, the overall values of microfracture density were higher than porosity. This is because the microfracture density reported both type of fractures: (1) fractures filled with secondary minerals like clay and calcite and (2) unfilled fractures. The abundance of microfractures (unfilled or filled

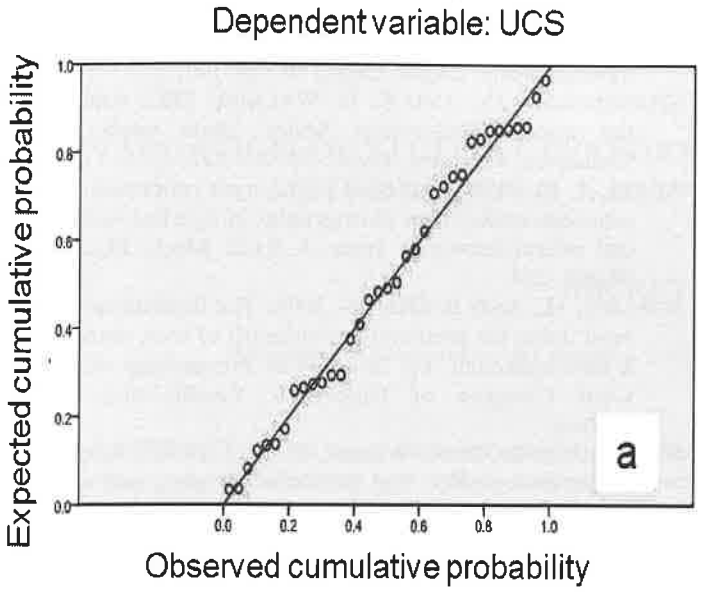

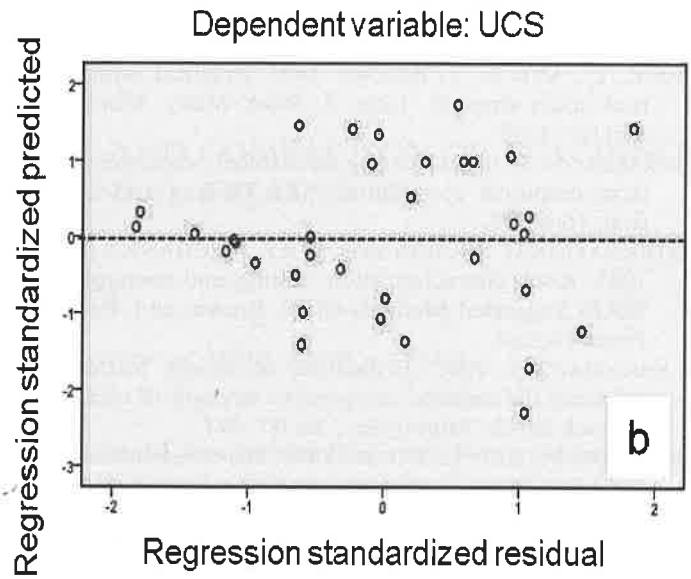

FIG. 4a. Normal P-P plot of regression Standardized residuals from the final multivariate regression result.
FIG. 4b. Scatter plots of regression standardized predicted versus regression standardized residuals.

with soft minerals) influenced the UCS of shale samples, a finding that was also supported by the multiple regression result. Specific gravity of shale is influenced by the presence of low density minerals like clay and the amount of unfilled spaces in the rock. The multiple regression output indicated that specific gravity influences the compressive strength of shale. Moisture content of the samples is an important factor that is known to influence the UCS of shale. In the study area, the moisture content of the shale was very low and was not comparable to porosity and microfracture density. The underlying reason may be that the shale samples were dry overall, with the only exception being microfractures filled with hygroscopic minerals that can absorb some moisture. The regression analysis discarded this factor before the final step of the iteration, as its presence was beyond the statistical significance of the overall model.

CONCLUSION

Weathered Ordovician-age Sevier Shale is widely distributed throughout the southern Appalachians. Thirty-five Sevier Shale samples were analyzed in the field and in laboratory in order to investigate the relationship between the mineralogy, microfacture density, physical behavior, and UCS. Backward multiple regression technique was performed to statistically evaluate and extract the significant variables.

Strong statistical correlation was observed between UCS and clay content, porosity, microfracture density, and the specific gravity of the shale, whereas the abundance of quartz, feldspar, and calcite showed no significant correlation with UCS. The presence of microfractures filled with clay and calcite in the rock significantly affected the strength of the rock. Overall porosity of the shale was low, and it was related to the microfracture density. Based on the PLI values, the UCS was calculated, ranging from weak to medium strong to strong rock. During the Point Load test, the fissile shale samples had a tendency to break along predefined planes of weakness; thus, the test was performed perpendicular to the fissile planes. Shale is anisotropic in nature, and the UCS of shale may vary with direction. In addition to the Point Load test, it would be reasonable to estimate UCS using Schmidt Hammer, Sonic Velocity, and standard compression test for comparison.

ACKNOWLEDGMENTS

The authors express sincere thanks to H. Moore, Geotechnical Engineer, Tennessee Department of Transportation, for providing relevant geotechnical data; C. Luitkus for the help in petrographical studies; Y. Liu for input in statistical evaluation; and K. Nandi and the anonymous reviewers for comments and suggestions.

LITERATURE CITED

ASTM. 1996. Standard test method for slake durability of shales and similar weak rocks: D464487. American Society for Testing Materials publication, West Conshohocken, Pennsylvania.

BROCH, E., AND J. A. FRANKLIN. 1972. The Point Load Strength Test. Inter. J. Rock Mech. Mining Sci., 9:669–697.

BROWN, E. T. 1981. Rock characterization, testing and monitoring. Pergamon Press, Oxford.

CHANG, C., M. ZOBACK, AND A. KHAKSAR. 2006. Empirical relations between rock strength and physical properties in sedimentary rocks. J. Petrol. Sci. Engin., 51:223–237.

DICK, J., AND A. SHAKOOR. 1992. Lithologic controls of mudrock durability. Quart. J. Engin. Geol. Hydrol., 25:31–46.

GEMICI, U. 2001. Durability of shales in Narlidere, Izmir, Turkey, with an emphasis on the impact of water on slaking behavior. Environ. Geol., 41:430–439.

GOKCEOGLU, C., AND H. AKSOY. 2000. New approaches to the characterization of clay-bearing, densely jointed and weak rock masses. Engin. Geol., 58:1–23.

HAYES, C. W. 1891. The overthrust faults of the southern Appalachians. Geol. Soc. Amer. Bull., 2:141–152.

HOEK, E., AND E. T. BROWN. 1997. Practical estimates of rock mass strength. Inter. J. Rock Mech. Mining Sci., 34:1165–1186.

HORSRUD, P. 2001. Estimating mechanical properties of shale from empirical correlations. SPE Drilling and Completion, 16:68–73.

INTERNATIONAL SOCIETY FOR ROCK MECHANICS [ISRM]. 1985. Rock characterization, testing and monitoring. *In* ISRM Suggested Methods (E. T. Brown, ed.). Pergamon Press, Oxford.

KAHRAMAN, S. 2001. Evaluation of simple methods for assessing the uniaxial compressive strength of rock. Inter. J. Rock Mech. Mining Sci., 38:981–994.

MARINOS, P., AND E. HOEK. 2006. The construction of the Egnatia Highway through unstable slopes in northern Greece. *In* Proceedings of XI Conference on Rock Mechanics (E. Hoek and P. Marinos, eds.). Turin, Italy.

RODGERS, J. 1953. Geologic Map of East Tennessee, with explanatory notes. State of Tennessee, Dept. of Conserv., Div. Geol. Bull., 58.

SANTI, P. 2006. Field methods for characterizing weak rock for engineering. Environ. Engin. Geosci., 12:1–11.

SHALABI, F. I., E. J. CORDING, AND O. H. AL-HATTAMLEH. 2007. Estimation of rock engineering properties using hardness tests. Engin. Geol., 90:138–147.

SHANMUGAM, G., AND K. R. WALKER. 1983. Anatomy of the middle Ordovician Sevier Shale basin, eastern Tennessee. Sediment. Geol., 34:315–337.

SINGH, S. K. 2001. Prediction of strength properties of some schistose rocks from petrographic properties using artificial neural networks. Inter. J. Rock Mech. Mining Sci., 38:269–284.

SONMEZ, H., AND B. OSMAN. 2008. The limitations of point load index for predicting of strength of rock material and a new approach. Pp. 261–264 *in* Proceedings of the 61st Geol. Congress of Turkey (S. Yazdir, ed.). Ankara, Turkey.

VALLEJO, L. E., R. A. WELSH, C. W. LOVELL, AND M. K. ROBINSON. 1993. The influence of fabric and composition on the durability of Appalachian Shales Rock for erosion control. American Society for Testing Materials publication; Special Tech. Pub. 1177, Philadelphia, Pennsylvania.

YASAR, E., AND Y. ERDOGAN. 2004. Estimation of rock physicomechanical properties using hardness methods. Engin. Geol., 71:281–288.